J Mater Sci (2010) 45:3381–3387
DOI 10.1007/s10853-010-4361-3

Density functional study of structural and electronic properties of GaP_n ($2 \le n \le 12$) clusters

Ling Guo

Received: 7 July 2009 / Accepted: 27 February 2010 / Published online: 16 March 2010

Abstract Low-lying equilibrium geometric structures of GaP_n ($n = 2$–12) clusters obtained by an all-electron linear combination of atomic orbital approach, within spin-polarized density functional theory, are reported. The binding energy, dissociation energy, and stability of these clusters are studied within the local spin density approximation (LSDA) and the three-parameter hybrid generalized gradient approximation (GGA) due to Becke–Lee–Yang–Parr (B3LYP). Ionization potentials, electron affinities, hardness, and static dipole polarizabilities are calculated for the ground-state structures within the GGA. It is observed that the gallium atoms of the symmetric ground-state structures prefer to occupy the peripheral positions. It is found that the relative ordering of the isomers is influenced by the nonlocal exchange-correlation effects for small clusters. Generalized gradient approximation extends bond lengths and widens the energy gap between the highest occupied molecular orbital (HOMO) and the lowest unoccupied molecular orbital (LUMO), as compared to the LSDA gap. The odd–even oscillations in the dissociation energy, the second differences in energy, the HOMO–LUMO gaps, the ionization potential, the electron affinity, and the hardness are more pronounced within the GGA. The stability analysis based on the energies clearly shows the GaP_5 and GaP_7 clusters to be endowed with special stabilities.

Introduction

Small clusters composed of phosphorus atom have been the subjects of intensive studies for the last two decades. A large number of studies of phosphorus clusters, both theoretical as well as experimental have been reported (see, for example, the reviews in Refs. [1–4]). One of the main motivations behind these studies is to understand the evolution of physical properties with the size of the cluster. Many properties of phosphorus clusters can be understood using the spherical jellium model (SJM), in which the ions are smeared out in a uniformly charged sphere leading to electronic shell closures for clusters containing a "magic" number 2, 8, 20, 40, 58, 92, 138 … of valence electrons. These findings were subsequently confirmed by first-principles theoretical calculations in which the ions were represented by pseudopotentials [5]. The question is the effect of doping by a single impurity on the electronic structure and geometry of these clusters. In bulk materials, a small percentage of impurity is known to affect the properties significantly. In clusters, the impurity effect should be even more pronounced and influenced by the finite size of the system. Taylor et al. [6–8] performed some experiments in this direction. They reported the experimental adiabatic electron affinity and vertical detachment energy of GaP_n ($n = 1$–4).

This experimental work triggered an interest in simulations of Ga-doped phosphorus clusters. Archibong et al. [9, 10] have reported the equilibrium geometries, harmonic vibration frequencies, and electron detachment energies of the neutral and anion GaP and GaP_2 performed at B3LYP-DFT and coupled cluster singles and doubles with connected triples [CCSD (T)] methods. Feng and Balasubramanian [11, 12] have also studied the structures and potential energy curves of electronic states of GaP_2, GaP_3,

---

L. Guo (✉)
School of Chemistry and Material Science, Shanxi Normal University, Linfen 041004, China
e-mail: gl-guoling@163.com

and its positive ions, using the complete active space self-consistent field (CASSCF) method followed by multireference singles and doubles configuration interaction (MRSDCI). Other theoretical studies on GaP_n have also been published [13].

To provide further insight on GaP_n clusters, I have carried out a detailed systematic study of the equilibrium structure and various electronic-structure-related properties of these clusters, employing both the local spin density (LSDA) and hybrid generalized gradient approximation (GGA) for the exchange–correlation potential, which is proved suitable for the gallium phosphide system [14–16]. I have investigated the relative ordering of these structures with the Ga impurity occupying the internal and peripheral position, and show that although the ground-state structures have Ga taking a peripheral position; these structures are energetically in competition with those where Ga occupies a central position. The calculations are explicitly carried out, to our knowledge for the first time, by considering all electrons in the calculations with no pseudopotentials (with nonlocal gradient corrections). Furthermore, the all-electron treatment eliminates issues like core-valence exchange-correlation, which occurs in the pseudopotential treatment when there is no marked distinction between the core and valence regions [17]. Here, evolution of the ionization potential, electron affinity, HOMO–LUMO gap, hardness, polarizability, dissociation energy, and binding energy for GaP_n clusters up to $n = 12$ have been studied. These physical quantities are compared with their counterparts calculated at the same level (all-electron B3LYP/6-311 + G*) for pure phosphorus clusters, which to our knowledge also represent the first all-electron with gradient corrections calculations in these systems.

In the following section, I briefly outline the computational methodology. In "Results and discussion" section the results are presented and discussed, and the conclusions are concluded in "Summary and conclusions" section.

Methodology and computational details

The geometry optimization and electronic-structure calculation are carried out using a molecular-orbital approach within the framework of spin-polarized density functional theory [18, 19]. An all-electron 6-311 + G* basis set [20] is employed, which is proved proper by Archibong et al. [9, 10]. I have employed KS exchange functional due to Slater in the local spin density approximation along with the Vosko–Wilk–Nussair [21] parametrization of homogeneous electron gas data due to Ceperley and Alder [22], for the correlation potential. I shall henceforth refer to this specific LSDA approach as SVWN. Calculations that go beyond the LSDA and take into account gradient corrections have also been carried out. In this case, Becke's three parameter functional (B3LYP) have been used, which use part of the Hartree–Fock exchange (but calculated with KS orbitals) and Becke's exchange functional in conjunction with the Lee–Yang–Parr [23, 24] functional for correlation. Frequency analysis is performed at the B3LYP/6-311 + G* level to check whether the optimized structures are transition states or true minima on the potential energy surfaces of corresponding clusters. The initial input structures are taken either from published results for P_n by adding Ga atoms in different positions, or the results reported for other III–V semiconductor clusters, or arbitrarily constructed and fully optimized via the Berny algorithm [25]. Symmetry constraints are removed whenever imaginary frequencies are found. Since one does not know a priori the spin multiplicity of the clusters, the above calculations are repeated for different spin configurations to obtain the lowest energy structure. All calculations are carried out using GAUSSIAN 98 [23] suite of programs.

Results and discussion

The geometries of all the clusters obtained within the LSDA and B3LYP are similar, apart from the larger bond distances observed in B3LYP, although the order of isomers is reversed in some cases with B3LYP. Therefore, Fig. 1 presents only the structures obtained within the B3LYP scheme.

The structural features of the GaP_n clusters have been discussed first. In the B3LYP scheme, the lowest-energy structure for GaP_2 is an isosceles triangular structure, with the Ga atom at the apex (a in Fig. 1), which is similar to elemental trimers P_3 [3]. Feng and Balasubramanian [11] reported a theoretical bond lengths of 2.658 and 1.960 Å for Ga–P and P–P bonds and a bond angle of 43.9° at the MRSDCI + Q level of theory with relativistic effective core potentials (RECPS) and 3s3p valence basis sets. Achibong et al. [9, 10] have optimized the geometry with $r_{\mathrm{Ga-P}} = 2.586$ Å, $r_{\mathrm{p-p}} = 1.989$ Å, $\theta_{\mathrm{PGaP}} = 45.2°$ at the MP2 level. Our B3LYP results ($r_{\mathrm{Ga-P}} = 2.678$ Å, $r_{\mathrm{p-p}} = 1.981$ Å, $\theta_{\mathrm{PGaP}} = 43.4°$) are close to the earlier MRSDCI + Q and MP2 results. A bent chain with C_s ($^2A''$) symmetry (b in Fig. 1) and a linear structure in which Ga take a terminal position, are two low-lying structures at, respectively, 0.66 and 0.68 eV above the most stable structure.

Three energetically close structures are found for GaP_3 in the B3LYP scheme. The most stable one has a C_s ($^1A'$) structure (a in Fig. 1) with the Ga impurity occupying a peripheral position. The other structure is a distorted rhombus (b in Fig. 1), and the energy is above the most stable one by 0.29 eV. A C_{3v} structure (not show) obtained

Fig. 1 Geometries of GaP_n structures

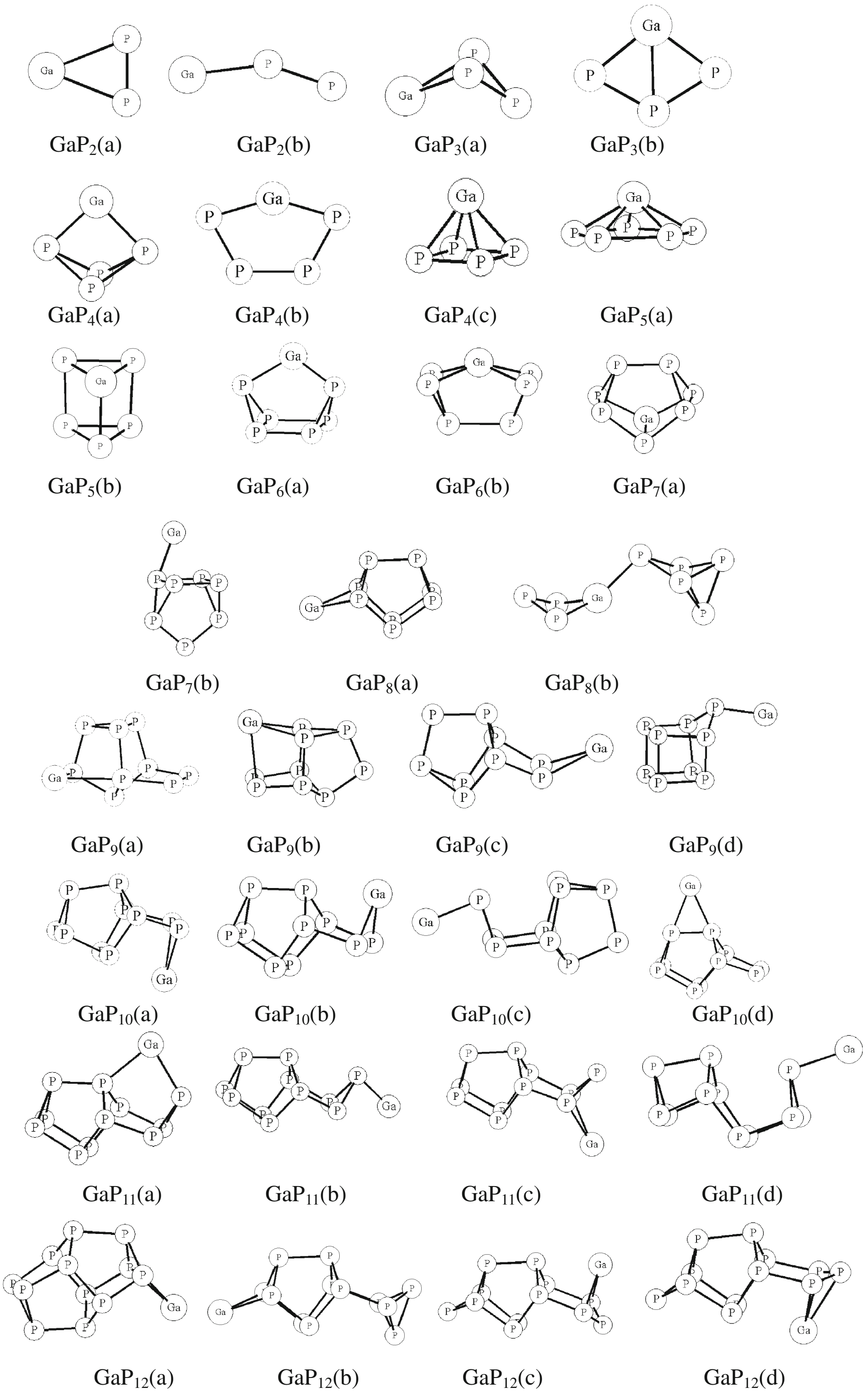

$GaP_2(a)$ $GaP_2(b)$ $GaP_3(a)$ $GaP_3(b)$

$GaP_4(a)$ $GaP_4(b)$ $GaP_4(c)$ $GaP_5(a)$

$GaP_5(b)$ $GaP_6(a)$ $GaP_6(b)$ $GaP_7(a)$

$GaP_7(b)$ $GaP_8(a)$ $GaP_8(b)$

$GaP_9(a)$ $GaP_9(b)$ $GaP_9(c)$ $GaP_9(d)$

$GaP_{10}(a)$ $GaP_{10}(b)$ $GaP_{10}(c)$ $GaP_{10}(d)$

$GaP_{11}(a)$ $GaP_{11}(b)$ $GaP_{11}(c)$ $GaP_{11}(d)$

$GaP_{12}(a)$ $GaP_{12}(b)$ $GaP_{12}(c)$ $GaP_{12}(d)$

by replacing a P atom in an apical position with a Ga atom in the tetrahedral P_4 [3] is another low-lying structure higher in energy by 0.36 eV.

In the case of GaP_4, three low-lying nearly degenerate structures are found, two of which are 3-D structure and the other one is planar. The ground state of the GaP_4 molecule is found to be the 3-D (C_{2v}, $^2A_1$) isomer (a in Fig. 1), which is similar to P_5 [3] and the valence-isoelectronic $GaAs_4$ [26]. There exists two kinds of P–P and one kind of Ga–P bonds in the neutral ground state, and the Ga–P bond lengths are longer than those for axial and equatorial P–P bonds by about 0.178 and 0.246 Å, respectively. A pentagon planar structure (b in Fig. 1) is higher in energy by 0.25 eV, which can be considered to replace a P atom in an apical position with a Ga atom in the structure of P_5 (a planar D_{5h} pentagon). And the square pyramid (C_{4v}, $^2A_1$) (c in Fig. 1) is above the lowest energy structure by 0.65 eV in energy.

The GaP_5 ground state has the high C_{5v} ($^1A_1$) symmetry (a in Fig. 1), which is derived from the P_5 cluster [3] by placing a five-fold Ga atom on the top. The other low-lying structure (b in Fig. 1) with the lower C_s ($^1A'$) symmetry is a distorted triangle prism lying 1.05 eV higher in energy. The Ga impurity in this geometry can be looked upon as the substitution impurity in the low-lying triangle prism P_6 [3] cluster.

The equilibrium lowest-energy geometry of GaP_6 (a in Fig. 1) is derived from a boat-shaped P_6 [3] by adding of one two-fold Ga atom between two P atoms. A face-capped triangle prism (b in Fig. 1) is higher in energy than the lowest-energy structure by 0.38 eV, which can be viewed as capping an additional Ga atom on the square face of the triangle prism P_6 [3].

The present calculations consider a cuneate structure as the ground state of GaP_7 cluster (a in Fig. 1), which can be derived from a square-face-capped triangle prism P_7 [3] by adding an additional three-fold Ga atom. The symmetry of P_7 is changed from C_{2v} to lower C_s ($^1A'$) symmetry of GaP_7 in the process. Next GaP_7 isomer in the energy ordering is a distorted cube structure (b in Fig. 1) with C_s ($^1A'$) symmetry lying 0.39 eV in energy above the ground state, which is obtained by substitution of one P atom by one Ga atom in the cube P_8.

The most stable geometry of GaP_8 is the result of the addition of the Ga atom to the lowest-energy structure of P_8 [3] cluster (a in Fig. 1). The C_s structure b in Fig. 1 is higher in energy by 0.88 eV.

The number of possible Ga adsorption structures increases rapidly with the cluster size. In spite of the large number of investigated configurations, I cannot, therefore, completely exclude the possibility that a more favorable structure does still exist. Figure 1 shows the most stable (a) and the more stable configurations (b–d) for each of the GaP_n ($n = 9$–12) complexes. Many clusters that the Ga atom started in each possible position of the parent pure phosphorus have been tried. From Fig. 1, we could find that the lowest-energy state of GaP_n structures for $n > 8$ are also results of capping the Ga impurity in a peripheral position of pure P_n clusters.

For GaP_9 cluster, the ground state geometry (a) is the Ga atom connecting with two P atoms of P_9 with C_1 symmetry. The structures of isomer (b), (c), and (d) are above the lowest-energy structure by 0.40, 0.81, and 1.00 eV, respectively, which could be also seen capping the different positions of the P_9 cluster.

The ground state geometry of GaP_{10} (a) with C_1 symmetry is the Ga atom substitute on capping P atom of P_{11} cluster. Another isomer (b), 0.48 eV higher than (a) can also be seen as substitution structure of P_{11}. Two low-lying isomers (c) and (d), which is building on the base of the structures of the P_{11}, are 0.51 and 0.94 eV, higher in energy, respectively.

For the case of GaP_{11}, the Ga atom capping the ground state structure of P_{11} cluster yields the lowest-lying structure for the GaP_{11} cluster (a). By adding the impurity Ga atom on another P atom, the low-lying structures (b) and (c) could be obtained, which are 0.13 and 0.53 eV higher than (a). And the energy difference of structure (d) and (a) is 0.92 eV.

The lowest-energy structure of GaP_{12} (a) is formed by capping the Ga atom on the ground-state structure of P_{12}.

Replacing the different edge P atom of P_{13} by Ga impurity, three substable geometries of GaP_{12} (b), (c), and (d) could be obtained. They are 0.55, 0.85, and 0.97 eV higher in energy.

In general, the P impurity in the most stable structures of GaP_n clusters can be looked upon as a substitution Ga impurity in pure P_{n+1} clusters [3] or capping the different sides of the low-lying geometry of P_n clusters [3], and the Ga impurity prefers to sit outside the P_n clusters in each GaP_n case.

The energy surface of a large molecule can be rather complex and there could be other stable minimums corresponding to geometries that are unexplored. Although the isomers of GaP_n clusters have been studied extensively and reported in this article, there can be no guarantee that other possible minima do not exist. Our results of geometry optimization are only predictions, and it would be of great interest to see more experimental studies being done on the system.

I now discuss the relative stability of these clusters by computing the energy that is indicative of the stability. The atomization or binding energy (BE) per atom, the dissociation energy (DE), and the second differences of energy are computed, respectively:

$$E_b[GaP_n] = nE[P] + E[Ga] - E[GaP_n]/(n+1), \tag{1}$$

$$\Delta E[GaP_n] = E[GaP_n] - E[GaP_{n-1}] - E[P], \tag{2}$$

$$\Delta^2 E[GaP_n] = E[GaP_{n+1}] + E[GaP_{n-1}] - 2E[GaP_n]. \tag{3}$$

The calculated binding energies are shown in Fig. 2. The binding energy increases rapidly from 3.18 eV (3.31 eV with LSDA) for GaP_2 to 4.30 eV (4.61 eV with LSDA) for GaP_{10}, with a small peak at GaP_{10}, and beyond it tends to saturate. The LSDA binding energies are larger than the B3LYP binding energies. This trend is consistent with the generally observed overbinding tendency within LSDA. The BE curve of pure phosphorus clusters calculated at the B3LYP/6-311 + G* level of theory is also shown in the same figure. Its comparison with the BE

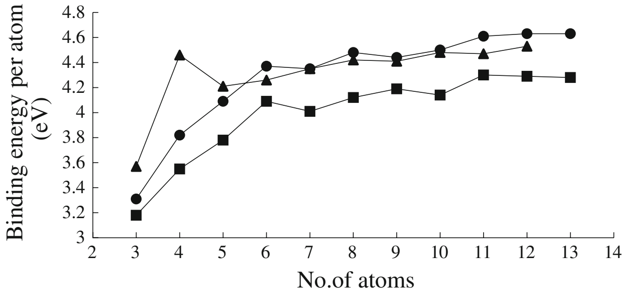

Fig. 2 Binding energy in electron volt: *squares* GaP_n with the B3LYP, *circles* GaP_n with the SVWN, *triangles* P_n with the B3LYP

curve for GaP_n clusters show that the small clusters of GaP_n are weakly bound. As the cluster grows in size, the difference between the BE curves of GaP_n clusters and pure phosphorus clusters diminishes steady, indicating that beyond GaP_4, the bonding in doped clusters is essentially similar to that in pure clusters.

The calculated values of the energy required for dissociation of GaP_n into $GaP_{n\text{-}1}$ and P are presented in Fig. 3. The LSDA values of dissociation energy are higher than their B3LYP counterpart, again indicating its overbinding nature. The curve shows odd–even oscillations with a peak for clusters with an even number of electrons for clusters $n < 9$, beyond which it do not exhibit odd–even pattern. The peak at GaP_5 is especially prominent.

In order to test the stability of cluster further, the following energy variation of reaction is considered:

$$2(GaP_n) \rightarrow (GaP_{n+1}) + (GaP_{n-1}).$$

The energy variation in formula (3) is defined as the second difference in energy for GaP_n. Hence, the curves shown in Fig. 4 are obtained. The larger the Δ^2E is, the more stable the cluster corresponding to the number of total atoms is. This curve again shows odd–even oscillation within $n < 9$ clusters, with peaks (dips) at an odd (even) number of phosphorus atoms. The peak at GaP_5 is conspicuous in both the LSDA and B3LYP schemes. The observation is consistent with that from the dissociation energies.

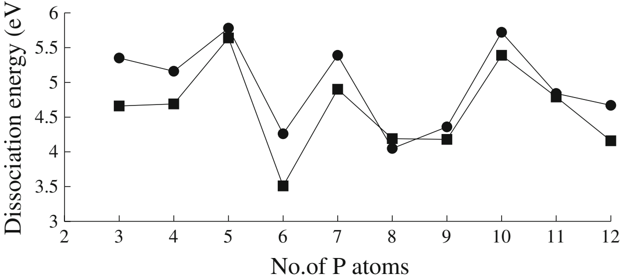

Fig. 3 Dissociation energy in electron volt: *squares* B3LYP, *circles* SVWN

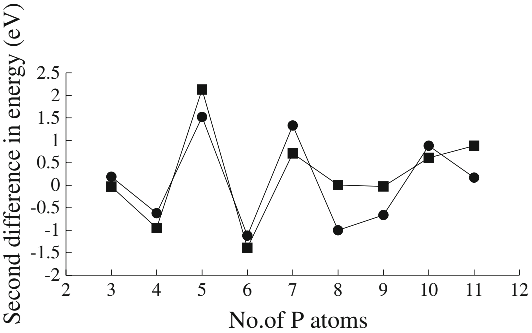

Fig. 4 Second difference in energy: *squares* B3LYP, *circles* SVWN

The adsorption energy of Ga, i.e., the energy released upon adsorption of Ga by a pure phosphorus cluster, has also been calculated, according to

$$E_{\text{ad}} = E[GaP_n] - E[P_n] - E[Ga]. \tag{4}$$

The calculated values of E_{ad} for the clusters up to P_{12} range between 1.03 and 3.49 eV (Table 1). The minimum value (1.03 eV) occurs for GaP_4, while it takes the maximum value (3.49 eV) for GaP_5.

The HOMO–LUMO gap is a useful quantity for examining the stability of clusters. It is found that systems with larger HOMO–LUMO gaps are, in general, less reactive. In the case of an odd-electron system, I calculate the HOMO–LUMO gap as the smallest spin-up–spin-down gap. The HOMO–LUMO gaps thus calculated are presented in Fig. 5. The HOMO–LUMO curve shows the same behavior in the LSDA and B3LYP schemes, and the peak at GaP_5, with 28 valence electrons, is prominent in both schemes. The clusters with an even number of electrons, with the exception of GaP_3, have peaks indicating their enhanced stability with respect to their neighbors.

Table 1 Adsorption energies (in eV) (see text for full details) calculated within B3LYP with (6-311 + G*) basis set

n	2	3	4	5	6	7	8	9	10	11	12
E_{ad}	1.42	3.48	1.03	3.49	2.49	2.48	1.78	1.64	1.91	2.31	1.34

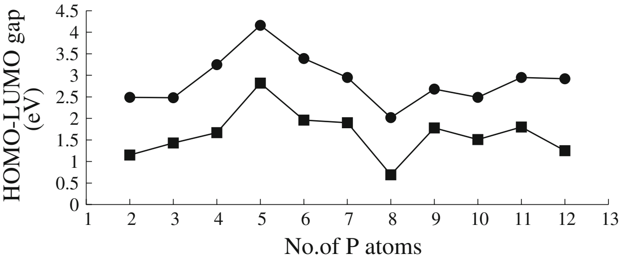

Fig. 5 HOMO–LUMO gap in electron volt: *squares* B3LYP, *circles* SVWN

Experimentally, the electronic structure is probed via measurements of ionization potentials, electron affinities, polarizabilities, etc. Therefore, these quantities are also been studied to understand their evolution with size. These quantities are determined within B3LYP for the lowest-energy structures obtained within the same scheme.

The vertical ionization potential (VIP) is calculated as the self-consistent energy difference between the cluster and its positive ion with the same geometry. The VIP is plotted in Fig. 6. As a function of cluster size. The VIP decreases as the cluster size increases, and shows oscillations with peaks for clusters with an even number of electrons. The peak occurring at GaP_5 is especially prominent, with large drops for the following clusters. Also shown in Fig. 6 are the VIPs of pure phosphorus clusters. These have also been calculated at the B3LYP/6-311 + G* level of theory, with structures optimized at the same level of theory. The comparison of the two curves shows that the GaP_n and P_n clusters exhibit the same odd–even pattern.

The vertical electron affinities (VEA) have also been calculated (see Fig. 7) by assuming the geometry for the charged cluster to be the same as for the neutral one. The VEA also exhibits an odd–even pattern. This is again a consequence of the electron pairing effect. In the case of clusters with an even number of valence electrons, the extra electron has to go into the next orbital, which costs energy, resulting in a lower value of VEA. A comparison of the VEAs of GaP_n clusters and pure phosphorus clusters again shows the same odd–even pattern. This observation is consistent with the observations from VIPs.

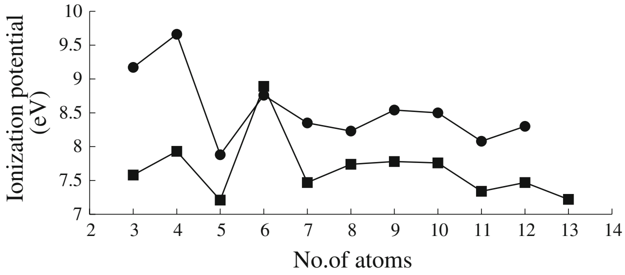

Fig. 6 Ionization potential in electron volt calculated at B3LYP/6-311 + G* level for GaP_n and P_n clusters: *squares* GaP_n clusters, *circles* P_n clusters

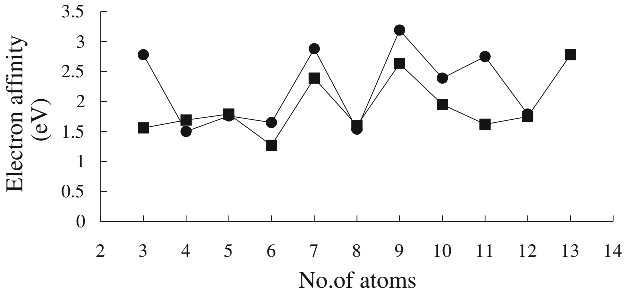

Fig. 7 Electron affinity in electron volt calculated at B3LYP/6-311 + G* level: *squares* GaP_n clusters, *circles* P_n clusters

Another useful quantity is the chemical hardness [19, 27, 28], which can be approximated as

$$\eta \approx 1/2(I - A), \tag{5}$$

where A and I are the electron affinity and ionization potential. Clusters with large values of hardness are, in general, less reactive and more stable. The hardness of GaP_n clusters, calculated according to Eq. 5 using VIP for the ionization potential and VEA for the electron affinity, is shown in Fig. 8. Chemical hardness has been established as an electronic quantity that in many cases may be used to characterize the relative stability of molecules and aggregates through the principle of maximum hardness (PMH) proposed by Pearson [29]. The PMH asserts that molecular systems at equilibrium present the highest value of hardness [30, 31]. Assuming that the PMH holds in these systems, I expect the hardness to present an oscillating behavior with local maxima at the clusters with even valence-electron clusters, as found for the VIP, VEA, and the relative energy in Fig. 4. Figure 8 shows that the even valence-electron clusters present higher values of hardness than their neighboring clusters. The even–odd oscillating feature could be observed, which is similar to that already stressed in the VIP, VEA, and stability criteria. Stable clusters are harder than their neighbors' odd valence-electron systems.

Table 2 presents the polarizabilities for the lowest-energy structures calculated within the B3LYP scheme. The polarizabilities per atom of GaP_n clusters decreases from 29.5 a.u. for GaP_2 to 25.3 a.u. for GaP_{12}, with the lowest value (24.4 a.u.) for GaP_7. The lowest value of polarizability per atom occurs for GaP_7, which could be due to a combined effect of the compactness of structure and the electronic shell closure that occurs for this cluster. The closed-shell electronic configuration of GaP_7 would result in the low response of the electrons to the applied electric field, resulting, thereby, in lower value of polarizability. Chattaraj et al. have proposed a minimum

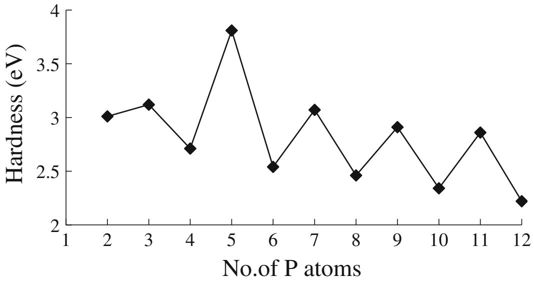

Fig. 8 Hardness of GaP_n clusters in electron volt calculated within the B3LYP

Table 2 Polarizabilities (in atomic units) calculated within the B3LYP with (6-311 + G*) basis set

System	α_{xx}	α_{yy}	α_{zz}	α	α/n
GaP_2	54.3	91.9	119.2	88.5	29.5
GaP_3	91.3	132.5	112.2	112.0	28.0
GaP_4	107.6	139.2	148.0	131.6	26.3
GaP_5	164.4	164.4	141.0	156.6	26.1
GaP_6	159.8	200.1	180.0	180.0	25.7
GaP_7	181.2	180.9	224.1	195.4	24.4
GaP_8	260.7	237.1	212.1	236.6	26.3
GaP_9	342.1	246.3	211.4	266.6	29.6
GaP_{10}	344.4	255.6	237.5	279.2	25.4
GaP_{11}	396.0	292.4	248.1	312.2	28.4
GaP_{12}	432.3	276.2	278.2	328.9	25.3

polarizability principle (MPP) [31–34], which states that the natural direction of evolution of any system is toward a state of minimum polarizability. There are many studies confirming the validity of the MPP on different kind of reactions and systems. Therefore, the GaP_7 cluster could be speculated the stable cluster. However, the conclusion should be proved in the future experiment. It is also evident from Table 2 that the odd–even oscillations, which are present in the binding energy, dissociation energy, VIP, VEA, and hardness, are not seen here.

Summary and conclusions

Phosphorus clusters doped with a single Ga impurity atom have been studied by an all-electron linear combination of atomic orbital approach, within spin-polarized density functional theory, using both the LSDA and hybrid GGA schemes for the exchange-correlation. A reversal of the order of isomers with LSDA and GGA occurs for small clusters with n. The Ga impurity is found to occupy a peripheral position. The stability of the lowest-energy structures is investigated by analyzing energies. Odd–even oscillations are observed in most of the physical properties investigated, suggesting that clusters with an even number of electrons are more stable than their odd-electron neighboring clusters. These odd–even effects are especially prominent within the B3LYP scheme. The stability analysis and the various electronic structure properties indicate an even valence-electron GaP_5 and GaP_7 clusters to be the most stable clusters among those studied.

Acknowledgements This work was financially supported by the National Natural Science Foundation of China (Grant No. 20603021), the Youth Foundation of Shanxi (Grant No. 2007021009), and the Youth Academic Leader of Shanxi.

References

1. Huang RB, Li HD, Lin ZY, Yang SH (1995) J Phys Chem 99:1418
2. Haser M, Schneide U, Ahlrichs R (1992) J Am Chem Soc 114:9551
3. Jones RO, Gantefor G, Hunsicker S, Pieperhoff P (1995) J Chem Phys 103:9549
4. Ballone P, Jones RO (1994) J Chem Phys 100:4941
5. Rothlisberger U, Andreoni W (1992) J Chem Phys 94:8129
6. Taylor TR, Asmis KR, Xu C, Neumark DM (1998) Chem Phys Lett 297:133
7. Taylor TR, Gomez H, Asmis KR, Neumark DM (2001) J Chem Phys 115:4620
8. Gomez H, Taylor TR, Zhao Y, Neumark DM (2002) J Chem Phys 117:8644
9. Archibong EF, St-Amant A (2000) Chem Phys Lett 316:151
10. Archibong EF, St-Amant A, Goh SK, Marynick DS (2002) Chem Phys Lett 361:411
11. Feng PY, Balasubramanian K (1997) Chem Phys Lett 265:41
12. Feng PY, Balasubramanian K (1998) Chem Phys Lett 288:1
13. Micic OI, Sprague JR, Curtis CJ, Jones KM, Machol JL, Nozik AJ, Giessen H, Fluegel B, Mohs G, Peyghambarian N (1995) J Phys Chem 99:7754
14. Costales A, Kandalam AK, Pandey R (2002) J Phys Chem B 106:1940
15. Costales A, Pandey R (2003) J Phys Chem A 107:191
16. Costales A, Kandalam AK, Pandey R (2003) J Phys Chem B 107:4508
17. Porezag D, Pederson MR, Liu AY (1999) Phys Rev B 60:14132
18. Parr RG, Yang W (1989) Density functional theory of atoms and molecules. Oxford, New York
19. Jones RO, Gunnarsson O (1989) Rev Mod Phys 61:689
20. Francl MM, Petro WJ, Hehre WJ, Binkley JS, Gordon MS, DeFrees DJ, Pole JA (1982) J Chem Phys 77:3654
21. Rao BK, Jena P (2000) J Chem Phys 113:1508
22. Ceperley DM, Alder B (1980) Phys Rev Lett 45:566
23. Frisch MJ, Trucks GW, Schlegel HB, Scuseria GE, Robb MA, Cheeseman JR, Zakrzewski VG, Montgomery JA, Stratmann RE, Burant JC, Dapprich S, Millam JM, Daniels AD, Kudin KN, Strain MC, Farkas O, Tomasi J, Baron V, Cossi M, Cammi R, Mennucci B, Pomelli C, Adamo C, Clifford S, Ochterski J, Petersson GA, Ayala PY, Cui Q, Morokuma K, Malick DK, Rabuck AD, Raghava-chari K, Foresman JB, Cioslowski J, Ortiz JV, Stefanov BB, Liu G, Liashenko A, Piskorz P, Komaromi I, Gomperts R, Martin RL, Fox DJ, Keith T, Al-Laham MA, Peng CY, Nanayakkara A, Gonzalez G, Challacombe M, Gill PMW, Johnson B, Chen W, Wong MW, Andres JL, Gonzalez C, Head-Gordon M, Replogle ES, Pople JA (1998) GAUSSIAN 98, Revision A.7. Gaussian, Inc., Pittsburgh, PA
24. Lee C, Yang W, Parr RG (1988) Phys Rev B 37:785
25. Becke AD (1988) Phys Rev A 38:3098
26. Piquini P, Canuto S, Fazzio A (1998) Nanostruct Mater 10:635
27. Parr RG, Pearson RG (1983) J Am Chem Soc 105:7512
28. Guo L, Wu HS, Jin ZH (2004) J Mole Struct 677:59
29. Pearson RG (1997) Chemical hardness: applications from molecules to solids. Wiley-VCH, Weinheim
30. Jaque P, Toro-Labbe A (2002) J Chem Phys 117:3208
31. Parr RG, Chattaraj PK (1991) J Am Chem Soc 113:1854
32. Chattaraj PK, Sengupta S (1996) J Phys Chem 100:16126
33. Chattaraj PK, Poddar A (1998) J Phys Chem A 102:9944
34. Chattaraj PK, Fuentealba P, Jaque P, Toro-Labbe A (1999) J Phys Chem A 103:9307